Nat. Hazards Earth Syst. Sci. Discuss., 1, 5033–5056, 2013
www.nat-hazards-earth-syst-sci-discuss.net/1/5033/2013/
doi:10.5194/nhessd-1-5033-2013

Natural Hazards and Earth System Sciences
Open Access
Discussions

A comparison of the measured North Sea Andrea rogue wave with numerical simulations

E. M. Bitner-Gregersen[1], **L. Fernandez**[2], **J. M. Lefèvre**[3], **J. Monbaliu**[2], **and A. Toffoli**[4,5]

[1]Det Norske Veritas AS, DNV Research and Innovation, 1322 Høvik, Norway
[2]Hydraulics Laboratory, Katholieke Universiteit Leuven, 3000 Leuven, Belgium
[3]Division Marine et Oceanographie, Meteo-France, Toulouse, France
[4]School of Marine Science and Engineering, Plymouth University, Drake Circus, Plymouth, PL4 8AA, UK
[5]Centre for Ocean Engineering Science and Technology, Swinburne University of Technology, P.O. Box 218, Hawthorn, VIC. 3122, Australia

Received: 25 August 2013 – Accepted: 2 September 2013 – Published: 25 September 2013

Correspondence to: E. M. Bitner-Gregersen (elzbieta.bitner-gregersen@dnv.com)

Published by Copernicus Publications on behalf of the European Geosciences Union.

Abstract

A coupling of a spectral wave model with a nonlinear phase resolving model is used to reconstruct the evolution of wave statistics during a storm crossing the North Sea on 8–9 November 2007. During this storm a rogue wave (named the Andrea wave) was recorded at the Ekofisk field. The wave has characteristics comparable to the well-known New Year wave measured by Statoil at the Draupner platform the 1 January 1995. Hindcast data of the storm are here applied as input to calculate random realizations of sea surface and evolution of its statistical properties associated with this specific wave event by solving the Euler equations with a Higher Order Spectral Method (HOSM). The numerical results are compared with the Andrea wave profile as well as characteristics of the Andrea wave record measured by the down-looking lasers at the Ekofisk field.

1 Introduction

A number of studies addressing rogue waves have been conducted theoretically, numerically, experimentally and based on the field data in the last decade. The occurrence of rogue waves, their generation mechanism, and detailed dynamic properties are now becoming clear. The state-of-the-art review on extreme and rogue waves can be found in recent review papers and books: Dysthe et al. (2008), Kharif et al. (2009), Osborne (2010), Slunayev (2010) and Onorato et al. (2013).

Predictions given by theoretical and numerical wave models accounting for nonlinearities beyond the second order in deep water such as: HOSM, Nonlinear Schrödinger Equations (NLS), the Dysthe model and the Conformal Method, compare well with experimental results (e.g. Onorato et al., 2006a; Shemer et al., 2010; Toffoli et al., 2010; Slunayev et al., 2012; Oberhagemann et al., 2012).

Unfortunately, there are still spare studies available based on field data, partly due to limited amount of rogue waves recorded in the ocean. Investigations of meteorological

NHESSD

1, 5033–5056, 2013

and oceanographic (met-ocean) conditions in which extreme and rogue waves occur together with analyses of field wave time series is of importance for getting better insight into mechanisms generating these abnormal waves.

It should be noted, however, that field data are usually recorded in 17–30 min every 3rd hour and therefore are affected by sampling variability (uncertainty due to limited number of observations) making more difficult to drawn firm conclusions from a field data analysis, see Bitner-Gregersen and Hagen (1990, 2003). Further, met-ocean conditions between each 3 h measurement are assumed to be stationary due to lack of information about their variability within the 3 h time period. There are some locations where continuous measurements of sea surface elevation are taken; however, they are still spare. It is important to note that sea states recorded continuously every 17–30 min usually are not remaining stationary not justifying therefore combination of 17–30 min wave records in one longer wave record. Thus sampling variability will also be present in 17–30 min wave records extracted from the continuous measurements and in statistical properties derived from them.

A long wave time series is needed to obtain reliable estimates of extreme values of sea surface elevation characteristics and their probability of occurrence being of importance for applications. The uncertainty due to sampling variability will particularly affect the higher order statistical moments like skewness and kurtosis which are more unstable than the estimates of significant wave height and spectral/zero-crossing wave period. To obtain reliable estimates of these higher order statistical moments at least 250–350 repetitions of a 17 min wave record will often be required, as demonstrated e.g. by Bitner-Gregersen and Hagen (2003). Therefore numerical wave models remain an important supporting tool in an analysis of field data.

As pointed out by Tomita (ISSC, 2009) both the numerical nonlinear wave models and the wave spectral models can be utilized in research of extreme and rogue waves and they are encouraged to be used. The complimentary nature of these models is clear; they give different information about a sea state. A spectral wave model (a WAM-type model) provides sea state description only in a form of the two-dimensional wave

NHESSD
1, 5033–5056, 2013

spectrum but does not give any information about the instantaneous position of the sea surface in a given sea state. Phase resolving wave models, on the other hand, give us the water surface elevation out of which statistical properties of individual waves can be extracted. Further, these nonlinear wave models allow simulation of a wave record for required time duration and by repeating the 17–30 min simulations significant reduction of uncertainty due to sampling variability in estimated sea surface characteristics and their probability of occurrence. Although the spectral wave model as well as the nonlinear numerical wave model is computationally intense, the great advance in enhancing computer power has made the coupling between these models feasible.

In the present study we demonstrate the complementary nature of the wave spectral model WAM and the numerical nonlinear wave model based on solving the Euler equations with the Higher Order Spectral Method (HOSM) proposed by West et al. (1987) by studying a storm named the Andrea storm crossing the central part of the North Sea on 8–9 November 2007. In this storm on 9 November 2007 a rogue wave called Andrea was recorded at the Ekofisk field (Magnusson and Donelan, 2013). This wave is comparable in characteristics, both with respect to the wave height and wave crest criterion, to the well-known New Year wave (called also the Draupner wave) measured by Statoil at the Draupner platform the 1 January 1995 (Haver and Andersen, 2000).

The paper is organized as follows: Sect. 2 describes the Andrea storm and the Andrea wave. Section 3 addresses hindcast data used in the analysis while Sect. 4 is dedicated to characteristics of the Andrea storm and comparison of numerical results to the measured values. Conclusions are summarized in Sect. 5.

2 The Andrea storm and the Andrea wave

A low entered the Northen North Sea on 8 November 2007. It covered Southern Norway and moved in the morning the 9 November towards Southern Sweden. Strong westerly wind (50–55 knots) followed the low and a high wave field (significant wave height of 10–11 m) was built up in the north area of the Ekofisk field (see Fig. 1) in the

NHESSD
1, 5033–5056, 2013

afternoon the 8 November 2007. The wind slightly decreased at Ekofisk around 18:00–21:00 UTC (from 22 m s^{-1} to 19 m s^{-1}). The strongest wind field passed the northeast and east of Ekofisk on the 9 November around 06:00 UTC and generated waves up to 11–12 m, for details see Magnusson and Donelan (2013).

The Andrea wave was recorded at Ekofisk by the down-looking lasers just past 00:00 UTC the 9 November 2007. This wave is comparable in characteristics to the well-known New Year wave (the Draupner wave) measured by Statoil at the Draupner platform the 1 January 1995 (Haver and Andersen, 2000). The Andrea wave characteristics, as reported by Magnusson and Donelan (2013), are compared to the New Year wave ones in Table 1. H_s denotes the significant wave height, T_p the spectral peak period, C_{max} the maximum crest height in the wave record, H_{max} the maximum zero-downcrossing wave height with the crest C_{max}, CF is the maximum crest factor (crest criterion), HF is the maximum height factor (height criterion).

CF > 1.3 (or > 1.2) and HF > 2 within a 20 min wave record represent simplified definitions of a rogue wave; see e.g. Bitner-Gregersen and Toffoli (2012). If both criteria are full filled a rogue wave is according to Krogstad et al. (2008) called a double rogue wave. As seen in Table 1 both the New Year wave as well as the Andrea wave can be called a double rogue wave. Note that both waves are recorded in the North Sea at the platforms located in the water depth of ca. 75 m.

3 Hindcast data

The hindcast data that are used in this study were retrieved from the European Centre for Medium Weather Forecast (ECMWF) archive. The data cover the period of the Andrea storm history from the 8 November 2007, 00:00 UTC to the 11 November 2011, 00:00 UTC and are stored at a sampling frequency of 6 h. The grid point from which the data have been extracted is located at the water depth of 74 m within a distance of ca. 50 km from the Ekofisk field. The data include the wind speed as well as the significant wave height and spectral peak period for the total sea, wind sea and swell.

NHESSD
1, 5033–5056, 2013

The components of the wind sea are those which are still under the influence of the local wind forcing and are detected as the part of wave spectrum where the wind input source term is positive. The remaining part of the wave spectrum is considered as swell (for details see, e.g. Hauser et al., 2005).

Figure 2 shows a history of the total significant wave height, spectral period and related sea state steepness, defined as $k_p H_s/2$ (k_p is the wavenumber at the spectral peak), during the Andrea storm. The significant wave height reaches the maximum at 06:00 UTC, 9 November 2007. This is consistent with the findings of Magnusson and Donelan (2013) based on the NORA10 hindcast data. The maximum wave height of 9.8 m is associated with the largest spectral peak period and the highest sea state steepness of 0.14 during the storm. It should be noted that the same high steepness is observed before the significant wave height reaches its maximum. Because the hindcast data are sampled every 6 h it is not possible to detect the steepness at 00:40 the 9 November 2007 when the Andrea wave is recorded at the Ekofisk field.

Probability of occurrence of rogue waves is related to mechanisms generating them. It is interesting to note that the output from a wave spectral model can be utilized when indicating a mechanism responsible for occurrence of a rogue wave, even though it may not always allow to reaching the firm conclusions. We illustrate it below for the Andrea wave.

The recognised mechanisms responsible for occurrence of rogue waves can be classified as follows (Onorato et al., 2006a, b, 2010, 2013; Toffoli et al., 2011; Didenkulova, 2010; Didenkulov and Pelinovsky, 2011; Sergeeva et al., 2011, 2013):

- linear Fourier superposition (frequency or angular linear focussing);
- wave–current interactions;
- crossing seas;
- quasi-resonance nonlinear interactions (modulational instability);
- shallow water effects.

NHESSD
1, 5033–5056, 2013

These mechanisms have also been considered in order to indicate a possible phenomenon responsible for occurrence of the Andrea wave.

The linear focusing is occurring very seldom and because the present study is addressing nonlinear waves the linear focusing has been eliminated from further considerations. Further, none strong current has been reported in the Ekofisk area representing the intermediate water depth ocean zone. Therefore wave-current interactions and shallow water effects seem not be responsible for occurrence of the Andrea wave.

The two remaining rogue wave generation mechanisms: crossing seas and quasi-resonance nonlinear interactions (modulational instability), could to be regarded as the only possible candidates which generated the Andrea wave. In order to select one of them the time history of wind sea and swell during the Andrea storm has been studied.

Figure 3 shows evolution of significant wave height for wind sea and swell during the Andrea storm. Wind sea dominates clearly the total sea during the growth, peak and decay of the storm. The significant wave height of swell is for the most of the time only slightly above 1 m, much lower than the wind sea significant wave height which reaches mostly 10 m at the peak of the storm. Therefore the total sea of the Andrea storm can be called the wind sea dominated one. The wind sea and swell has approximately the same energy (the significant wave height around 1 m) only at the start and the end of the storm.

It is well established that two wave trains with similar energy and frequencies travelling at particular angles can trigger modulational instability and be responsible for the formation of rogue waves, Onorato et al. (2006a, 2010). Such results have been confirmed through recent numerical simulations of the Euler equations and experimental work performed in the MARINTEK Laboratories, Toffoli et al. (2011). The investigations have shown that the kurtosis, a measure of the probability of occurrence of extreme waves, depends on an angle β between the crossing wave systems. The maximum value of kurtosis has been achieved for $40 < \beta < 60$. None such conditions where wind sea and swell has the same energy and spectral peak frequency and are crossing each other under the angle $40 < \beta < 60$ have been identified in the ECMWF hindcast data

NHESSD
1, 5033–5056, 2013

from the Andrea storm. The hindcast data seems to point out that the Andrea wave might have occurred in the sea state more prone to extreme waves as a result of modulational instability (i.e. the sea state with relative high steepness and not particularly broad spectrum).

This conclusion is supported by Fig. 4 presenting evolution of the directional wave spectrum during the Andrea storm at the location considered. One wave system is seen in the period 8 November 2007, 18:00 UTC–9 November 2007, 06:00 UTC, within which the Andrea wave was recorded.

4 Numerical simulations

Numerical simulations have been carried out to get further insight into the Andrea storm's characteristics. Short-term wave records at the 6 h sampling interval have been generated by solving the equations with the Higher Order Spectral Method (HOSM) as proposed by West et al. (1987).

In the case of constant water depth ($h = 74$ m in this study), the velocity potential $\Phi(x, z, t)$ of an irrotational, inviscid, and incompressible liquid satisfies the Laplace's equation everywhere in the fluid. The boundary conditions are such that the vertical velocity at the bottom ($z = -74$ is zero, and the kinematic and dynamic boundary conditions are satisfied for the velocity potential $\Psi(x, y, t) = \Phi(x, y, \eta(x, y, t), t)$ on the free surface, i.e., $z = \eta(x, y, t)$ (see Zakharov, 1968). The expressions of the kinematic and dynamic boundary conditions are as follows:

$$\Psi_t + g\eta + \frac{1}{2}\left(\Psi_x^2 + \Psi_y^2\right) - \frac{1}{2}W^2\left(1 + \eta_x^2 + \eta_y^2\right) = 0 \quad (1)$$

$$\eta_t + \Psi_x\eta_x + \Psi_y\eta_y - W\left(1 + \eta_x^2 + \eta_y^2\right) = 0 \quad (2)$$

where the subscripts denote the partial derivatives, and $W(x, y, t) = \Phi_z|\eta$ represents the vertical velocity evaluated at the free surface.

NHESSD
1, 5033–5056, 2013

The time evolution of an initial surface elevation can be calculated from Eqs. (1) and (2). For this study, we have used the Higher Order Spectral Method (HOSM), which was independently proposed by West et al. (1987) and Dommermuth and Yue (1987). A comparison of these two approaches (Clamond et al., 2006) has shown that the formulation proposed by Dommermuth and Yue (1987) is less consistent than the one proposed by West et al. (1987); the latter, therefore, has been applied herein. The advantage of HOSM in comparison to others methods is that it allows simulating a large number of random realizations of the surface elevation, within a reasonable computational time, without limitations in terms of the spectral bandwidth.

HOSM uses a series expansion in the wave slope of the vertical velocity $W(x, y, t)$ about the free surface. In the present study we have considered a third-order expansion so that the four-wave interaction is included (see Tanaka, 2001, 2007). With this assumption the solution presented is not fully nonlinear. The expansion is then used to evaluate the velocity potential $\Psi(x, y, t)$ and the surface elevation $\eta(x, y, t)$ from Eqs. (1) and (2) at each instant of time. The time integration is performed by means of a four-order Runge–Kutta method with a time step $\Delta t = T_p/200$ (T_p is the spectral peak period). All aliasing errors generated in the nonlinear terms are removed (see West et al., 1987; Tanaka, 2001, for details).

The HOSM simulations require as input an initial sea surface with periodic boundary conditions. This is calculated starting from the hindcast directional spectrum $E(\omega, \theta)$ by converting it into a wavenumber spectrum $E(k_x, k_y)$ with the linear dispersive relation, and then applying the inverse Fourier transform with the random amplitude and phase approximation. The converted spectrum, however, does not ensure constant Δk_x and Δk_y, which are needed for a period surface. Furthermore, standard output spectra only contain a very limited amount of frequencies and the resulting surface would be too course for statistical analysis. Therefore, in order to force periodic boundaries and refine the surface, wavenumbers are redefined by subdividing the domain 0 to k_{max} into a much larger number of modes spaced at constant intervals. The concurrent values of energy are obtained by simple linear interpolation. Note that this procedure may induce

NHESSD
1, 5033–5056, 2013

a shift in the peak period if the number of modes is not large enough. This is due to the fact that the new wavenumbers may not necessarily coincide with the original modes. To overcome this difficulty, 256 modes were applied in the present analysis to maintain unchanged the peak period.

In the definition of the initial surface, Δx and Δy were selected in order to ensure 10 wavelengths in the physical domain. The initial surface has been let to evolve according to Eqs. (1) and (2) for 70 peak periods. In order to have statistically significant results, 150 repetitions of the wave surface with different sets of random amplitudes and phases (see e.g. Toffoli et al., 2008) for the initial surface have been simulated.

Figures 4 and 5 show evolution of the directional wave spectrum in the period 8 November 2007, 00:00 UTC–10 November 2007, 18:00 UTC, covering the Andrea storm history. The spectra presented in the figures have been an input to the present simulations.

Time histories of the crest ratio CF = C_{max}/H_s, skewness and kurtosis in the period 8–11 November 2007 are shown in Fig. 6 (A_{max} denotes the maximum amplitude equal to C_{max}). The maximum crest ratio $C_{max}/H_s = 1.4$ corresponding to the kurtosis value of 3.35 is obtained at the location considered being in approximately the 50 km distance from the Ekofisk field. The ratio $C_{max}/H_s = 1.4$ is comparable to the one characterising the Andrea wave $C_{max}/H_s = 1.63$ recorded at the Ekofisk field (see Table 1), however, not as high.

It is interesting to note that the sea states being able to trigger rogue waves occur several times during the Andrea storm history at the location considered. North Seas scatter diagrams of H_s and T_p indicate that sea states with similar steepness do not occur very seldom in the North Sea. However, it should be noted that scatter diagrams provide limit description of sea states as they do not give any information about the frequency-directional wave spectrum.

Temporal evolution of skewness, kurtosis and A_{max}/A_0 (A_0 denotes the initial amplitude used in the simulations while A_{max} is the maximum amplitude (crest)) within the 70 T_p time period at different time points during the Andrea storm is shown in Figs. 7–9,

NHESSD
1, 5033–5056, 2013

respectively. The 70 T_p time period is not sufficient to include the time when the Andrea wave was recorded at the Ekofisk, the 9 November 2007, 00:40 UTC. At the location considered the maximum kurtosis is observed already after 30 T_p s simulations the 8 November 2007, 18:00 UTC. The location used in the analysis is not the same as the Ekofisk one therefore the kurtosis and wave crest could reach their maximum prior to the time of the occurrence of the Andrea wave at Ekofisk.

5 Conclusions

The investigations show how the wave spectral model WAM and the numerical HOSM wave model can be combined in investigations of extreme and rogue waves. The complimentary nature of these wave models is demonstrated by studying the Andrea storm which passed the Northern North Sea in November 2007. The results obtain agree satisfactory with the observations recorded at the Ekofisk field.

A spectral model coupled with the HOSM provides statistical information about sea states based on the actual hindcast/forecast spectrum, whether this is bimodal or unimodal. The output from the wave spectral model combined with the HOSM numerical simulations can give description of sea surface elevation, the maximum wave crest, skewness and kurtosis when rogue waves are present. The proposed approach is of general character and can be applied to investigations of any other storm. It represents a good supporting tool for an analysis of field data.

It needs to be noted that HOSM cannot be applied for prediction of rogue waves for very steep sea states because it does not include wave breaking. Although the wave spectral model like WAM provides valuable input to HOSM simulations the commonly used 6 h sampling interval may present a limitation when studying extreme and rogue waves. Important information between sampling intervals maybe missed.

The analysis shows that when the Andrea storm is passing the North Sea rogue waves can be expected in several locations, not only at Ekofisk where the Andrea wave was recorded. Rogue waves are deducted during the storm development; when

NHESSD
1, 5033–5056, 2013

storm builds up and when it decades, also in the location considered by the study being approximately 50 km from the Ekofisk field. They have not been observed when the storm reaches the largest H_s.

Uncertainties associated with the WAM and HOSM model, which will affect the presented results, have not been investigated in this study. Further investigations are still called for to evaluate impact of these uncertainties on extreme and rogue wave predictions.

The approach presented coupling the wave spectral model with the nonlinear phase resolving model can be considered to be used for forecasting purposes. Although these models are computationally intense, the great advance in enhancing computer power has made the coupling between them feasible.

Acknowledgements. This work has been supported by E.U. project EXTREME SEAS (SCP8-GA-2009-234175). F.W.O. project G.0333.09 is also acknowledged. L. Fernandez and J. Monbaliu also acknowledge the Hercules Foundation and the Flemish Government department EWI for providing access to the Flemish Supercomputer Center. E. M. Bitner-Gregersen and A. Toffoli thank Miguel Onorato and Carlo Brandini for fruitful discussions.

References

Bitner-Gregersen, E. M. and Hagen, Ø.: Uncertainties in data for the offshore environment, Struct. Safety, 7, 11–34, doi:10.1016/0167-4730(90)90010-M, 1990.

Bitner-Gregersen, E. M. and Hagen, Ø.: Effects of two-peak spectra on wave crest statistics, in: Proc. 22nd International Conference on Offshore Mechanics and Arctic Engineering (OMAE), Cancun, Mexico, 2003.

Clamond, D., Francius, M., Grue, J., and Kharif, C.: Long time interaction of envelope solitons and freak wave formations, Eur. J. Mech. B/Fluids, 25, 536–553, 2006.

Didenkulova, I.: Shapes of freak waves in the coastal zone of the Baltic Sea (Tallinn Bay), Boreal Environ. Res., 16, 138–148, 2010.

Didenkulov, I. and Pelinovsky, E.: Rogue waves in nonlinear hyperbolic systems (shallow-water framework), Nonlinearity, 24, R1–18, 2011.

NHESSD

1, 5033–5056, 2013

Dommermuth, D. G. and Yue, D. K.: A high-order spectral method for the study of nonlinear gravity waves, J. Fluid Mech., 184, 267–288, 1987.
Dysthe, K., Krogstad, H. E., and Müller, P.: Oceanic rogue waves, Ann. Rev. Fluid Mec., 40, 287–310, 2008.
Hauser, D., Kahma, K. K., Krogstad, H. E., Lehner, S., Monbaliu, J., and Wyatt, L. W. (Eds.): Measuring and analysing the directional spectrum of ocean waves, Cost Office, Brussels, 2005.
Haver, S. and Andersen, O. J.: Freak waves: rare realizations of a typical population or typical realizations of a rare population, in: Proc. 10th International Offshore and Polar Engineering (ISOPE) Conference, Seattle, USA, 2000.
ISSC 2009: Tomita, H.: ISSC 2009 I.1 Environment, Official Discusser, in: Proc. 17th International Ship and Offshore Structures Congress (ISSC), 3, Seoul, Korea, 2009.
Kharif, C., Pelinovsky, E., and Slunyaev, A.: Rogue waves in the ocean, in: Advances in Geophysical and Environmental Mechanics and Mathematics, Springer, Berlin, 11–31, 2009.
Oberhagemann, J., Ley, J., and el Moctar, O.: Prediction of ship response statistics in severe sea conditions using RANSE, in: Proc. 31th International Ocean, Offshore and Arctic Engineering (OMAE) Conference, Rio de Janeiro, Brazil, 2012.
Onorato, M., Osborne, A., Serio, M., Cavaleri, L., Brandini, C., and Stansberg, C.: Extreme waves, modulational instability and second order theory: wave flume experiments on irregular waves, Eur. J. Mech. B/Fluids, 25, 586–601, 2006a.
Onorato, M., Osborne, A., and Serio, M.: Modulation instability in crossing sea states: a possible mechanism for the formation of freak waves, Phys. Rev. Lett., 96, 014503, doi:10.1103/PhysRevLett.96.014503, 2006b.
Onorato, M., Proment, D., and Toffoli, A.: Freak waves in crossing seas, Eur. Phys. J., 185, 45–55, 2010.
Onorato, M., Residori, S., Bortolozzo, U., Montina, A., and Arecchi, F. T.: Rogue waves and their generating mechanisms in different physical contexts, Phys. Rep., 528, 47–89, 2013.
Osborne, A. R.: Nonlinear ocean waves and the inverse scattering transform, International Geophysics Series, Elsevier, San Diego, 2010.
Shemer, L., Sergeeva, A., Slunyaev, A.: Applicability of envelope model equations for simulation of narrow-spectrum unidirectional random field evolution: experimental validation, Phys. Fluids, 22, 016601, doi:10.1063/1.3290240, 2010.

NHESSD
1, 5033–5056, 2013

Slunyaev, A.: Freak wave events and the wave phase coherence, Eur. Phys. J. Spec. Top., 185, 67–80, 2010.
Slunyaev, A. V., Sergeeva, A., Pelinovsky, E. N.: Modelling of deep-water rogue waves: different frameworks, in: CENTEC Anniversary Book. Marine Technology and Engineering, edited by: Guedes Soares, C., et al., Taylor & Francis Group, London, 199–216, 2012.
Tamura, H., Waseda, T., and Miyazawa, Y.: Freakish sea state and swell-windsea coupling: numerical study of the Suwa-Maru incident, Geophys. Res. Lett., 36, L01607, doi:10.1029/2008GL036280, 2009.
Tanaka, M.: Verification of Hasselmann's energy transfer among surface gravity waves by direct numerical simulations of primitive equations, J. Fluid Mech., 444, 199–221, 2001.
Tanaka, M.: On the role of resonant interactions in the short-term evolution of deep-water ocean spectra, J. Phys. Oceanogr. 37, 1022–1036, 2007.
Toffoli, A., Bitner-Gregersen, E., Onorato, M., and Babanin, A. V.: Wave crest and trough distributions in a broad–banded directional wave field, Ocean Eng., 35, 1784–1792, 2008.
Toffoli, A., Gramstad, O., Trulsen, K., Monbaliu, J., Bitner-Gregersen, E. M., and Onorato, M.: Evolution of weakly nonlinear random directional waves: laboratory experiments and numerical simulations, J. Fluid Mech., 664, 313–336, 2010.
Toffoli, A., Bitner-Gregersen, E. M., Osborne, A. R., Serio, M. Monbaliu, J., and Onorato, M.: Extreme waves in random crossing seas: laboratory experiments and numerical simulations, Geophys. Res. Lett., 38, L06605, doi:10.1029/2011GL046827, 2011.
West, B. J., Brueckner, K. A., Jand, R. S., Milder, D. M., and Milton, R. L.: A new method for surface hydrodynamics, J. Geophys. Res., 92, 11803–11824, 1987.
Zakharov, V.: Stability of period waves of finite amplitude on surface of a deep fluid, J. Appl. Mech. Tech. Phys., 9, 190–194, 1968.

NHESSD
1, 5033–5056, 2013

Table 1. Characteristics of the Andrea and New Year waves.

Wave parameters	Andrea wave	Draupner wave
H_s	9.2 m	11.9 m
T_p	13.2 s	14.4 s
C_{max}	15.0 m	18.5 m
CF = C_{max}/H_s	1.63	1.55
H_{max}	21.1 m	25.0 m
HF = H_{max}/H_s	2.3	2.1

NHESSD
1, 5033–5056, 2013

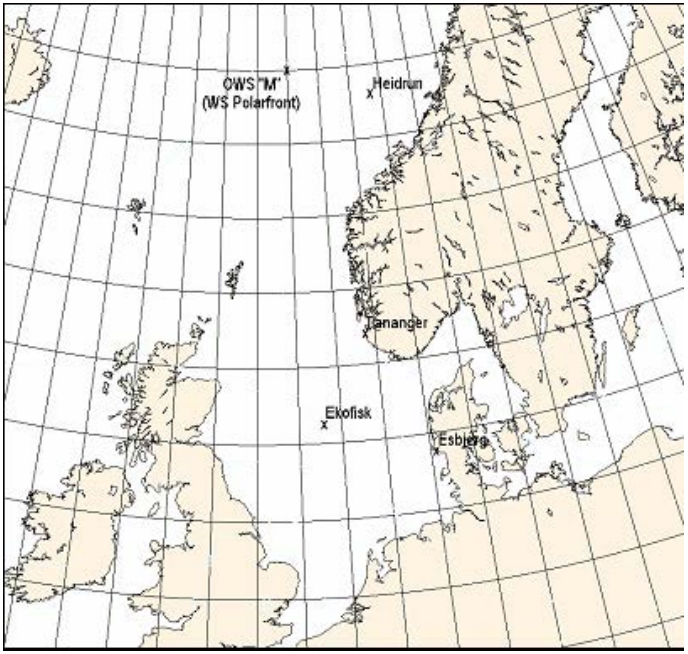

Fig. 1. Location of the Ekofisk field.

NHESSD
1, 5033–5056, 2013

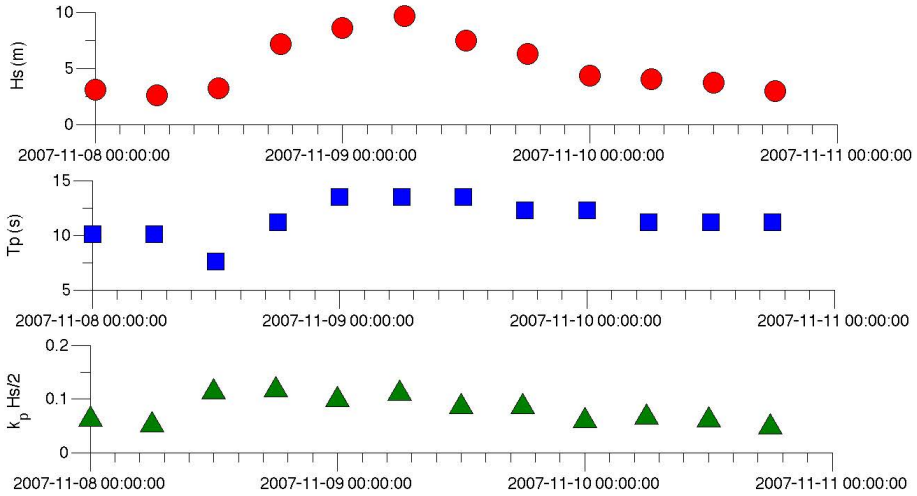

Fig. 2. History of significant wave height, spectral wave period and sea state steepness for the total sea during the Andrea storm.

NHESSD
1, 5033–5056, 2013

The Andrea wave and numerical simulations

E. M. Bitner-Gregersen et al.

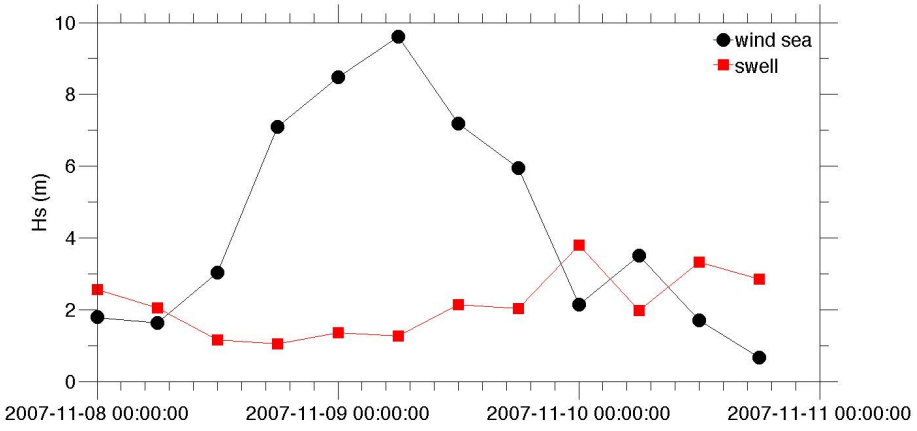

Fig. 3. History of significant wave height for wind sea and swell during the Andrea storm.

NHESSD
1, 5033–5056, 2013

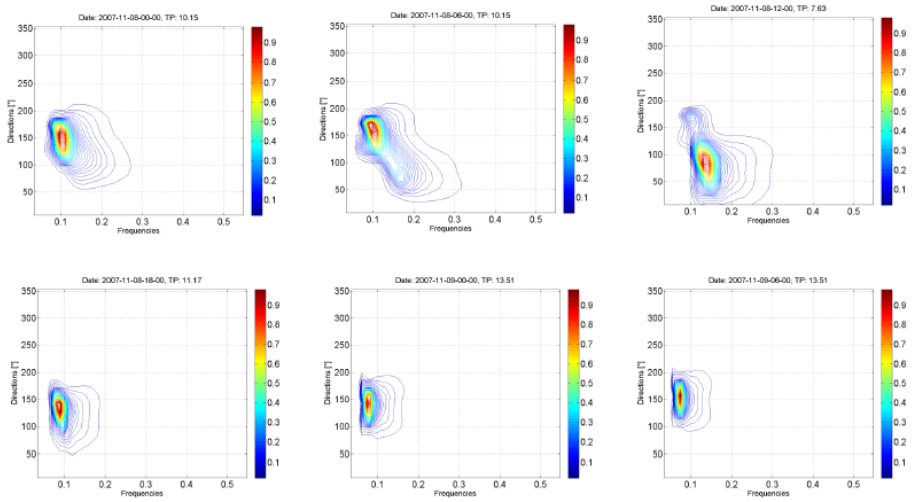

Fig. 4. Evolution of the directional wave spectrum during the Andrea storm, from 8 November 2007, 00:00 UTC, to 9 November 2007, 06:00 UTC.

NHESSD
1, 5033–5056, 2013

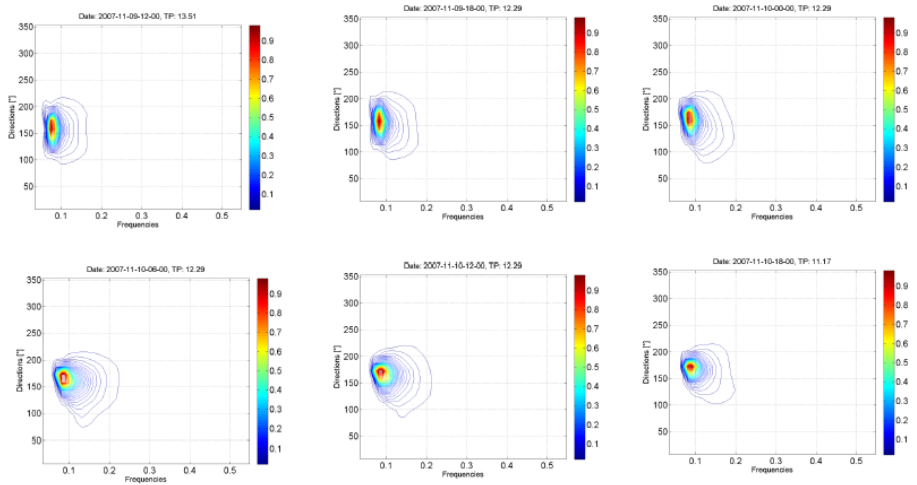

Fig. 5. Evolution of the directional wave spectrum during the Andrea storm, from 9 November 2007, 12:00 UTC, to 10 November 2007, 18:00 UTC.

NHESSD
1, 5033–5056, 2013

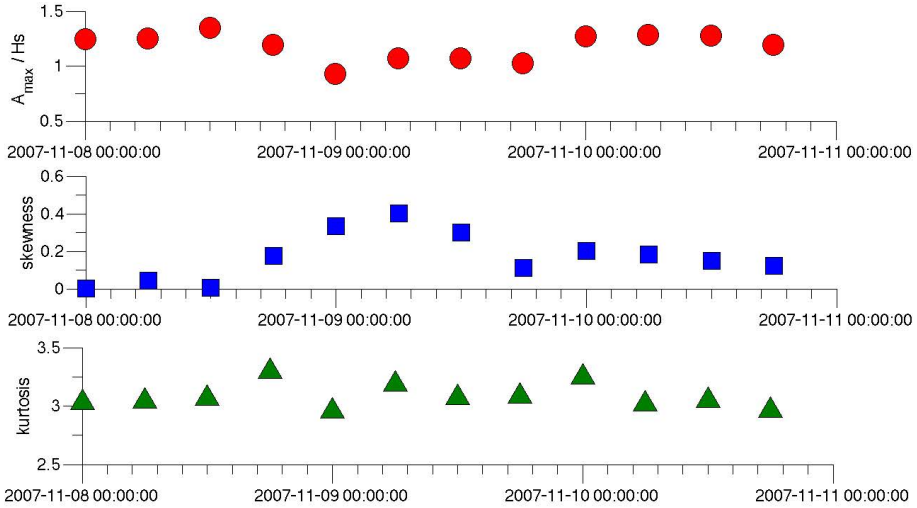

Fig. 6. Time histories of the crest ratio CF = C_{max}/H_s, skewness and kurtosis in the period 8–11 November 2007 (A_{max} is the maximum amplitude equal to C_{max}).

NHESSD
1, 5033–5056, 2013

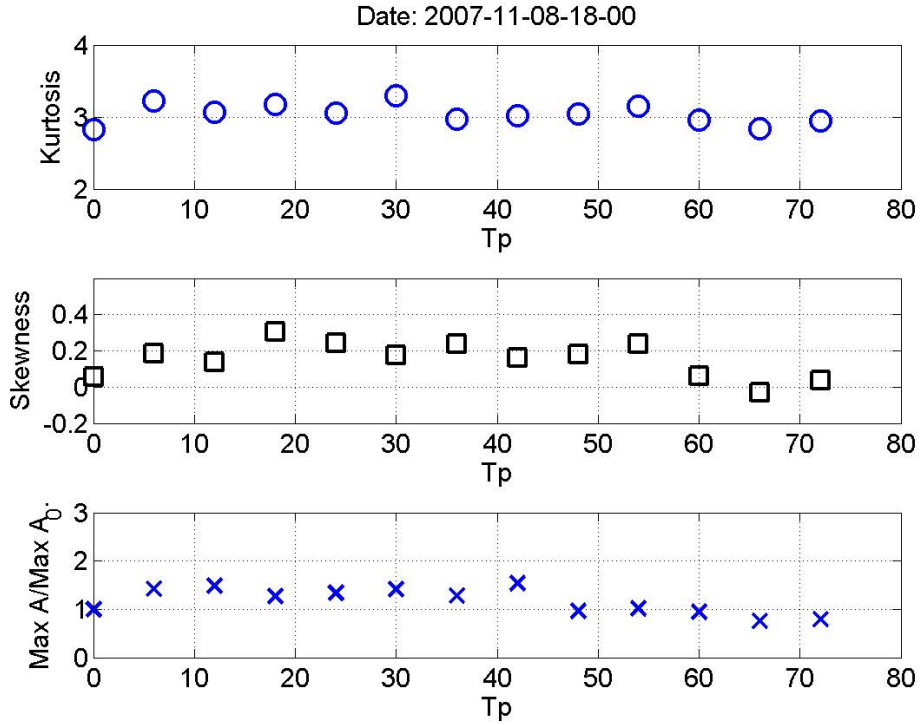

Fig. 7. Temporal evolution of skewness, kurtosis and A_{max}/A_0 (A_0 denotes the initial amplitude used in the simulations while A_{max} is the maximum amplitude (crest)), 8 November 2007, 18:00 UTC.

NHESSD
1, 5033–5056, 2013

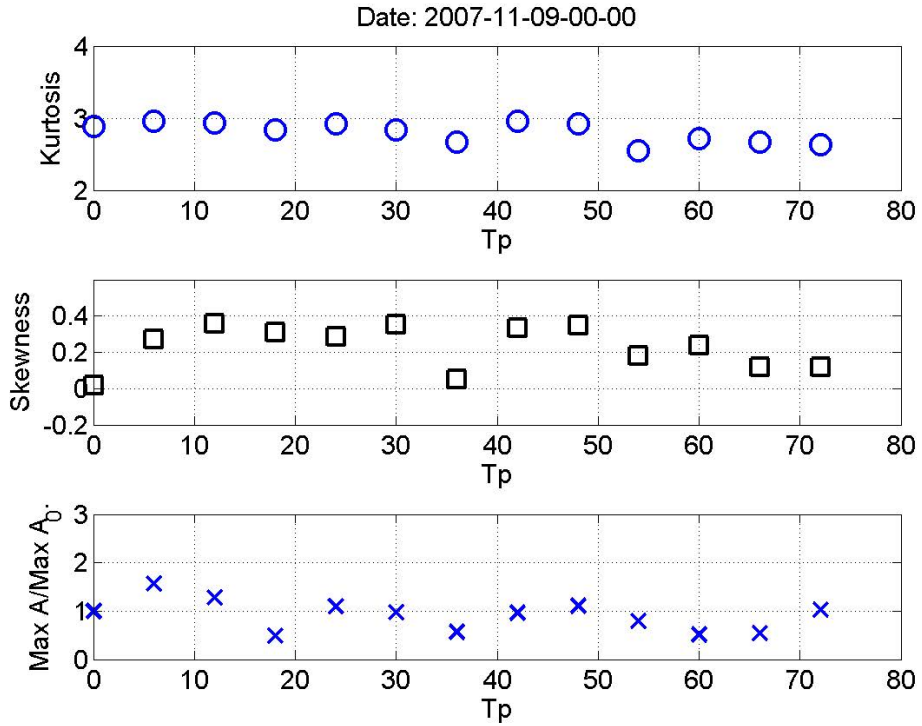

Fig. 8. Temporal evolution of skewness, kurtosis and A_{max}/A_0 (A_0 denotes the initial amplitude used in the simulations while A_{max} is the maximum amplitude (crest)), 9 November 2007, 00:00 UTC.

NHESSD
1, 5033–5056, 2013

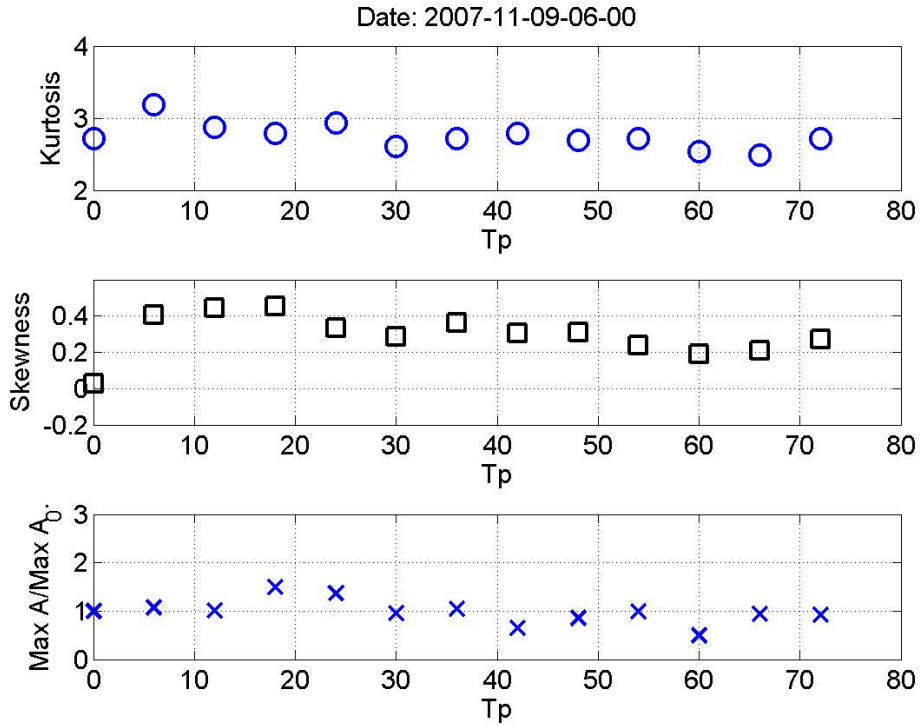

Fig. 9. Temporal evolution of skewness, kurtosis and A_{max}/A_0 (A_0 denotes the initial amplitude used in the simulations while A_{max} is the maximum amplitude (crest)), 9 November 2007, 06:00 UTC.

NHESSD
1, 5033–5056, 2013